The torque equation then becomes

$$\mathbf{L}(R^3/3K) = i(I_3 - I_2)[\beta_1\gamma_1 \cos^2\Phi + \beta_2\gamma_2 \sin^2\Phi + (\beta_1\gamma_2 + \beta_2\gamma_1) \cos\Phi \sin\Phi] + j(I_1 - I_3) \times [\alpha_1\gamma_1 \cos^2\Phi + \alpha_2\gamma_2 \sin^2\Phi + (\alpha_2\gamma_1 + \alpha_1\gamma_2) \cos\Phi \sin\Phi] + k(I_2 - I_1)[\alpha_1\beta_1 \cos^2\Phi + \alpha_2\beta_2 \sin^2\Phi + (\alpha_1\beta_2 + \alpha_2\beta_1) \cos\Phi \sin\Phi] \quad (A4)$$

When the angles θ_1, θ_2, θ_3 are small deviations from the reference axes, the torque reduces to the following components:

$$L_1 = 3\omega_0^2(I_3 - I_2)(\theta_1 \cos^2\Phi + \theta_3 \sin\Phi \cos\Phi)$$

$$L_2 = 3\omega_0^2(I_3 - I_1)(\theta_2 \cos^2\Phi - \theta_2 \sin^2\Phi + \sin\Phi \cos\Phi) \quad (A5)$$

$$L_3 = 3\omega_0^2(I_1 - I_2)(\theta_3 \sin^2\Phi + \theta_1 \sin\Phi \cos\Phi)$$

For the symmetric gyro of case 3, $I_1 = I_3 = A$ and $I_2 = C$, and the torque about axis 3 reduces to

$$L_3 = \tfrac{3}{2}\omega_0^2(A - C)\theta_3(1 - \cos 2\Phi) \quad (A6)$$

References

[1] Evans, H. W., "Analysis of one and two-gimbal attitude gyros in a satellite application," Rept. SM-39040, Douglas Aircraft Co., Inc., Santa Monica, Calif. (October 25, 1961).

[2] Thomson, W. T., "Spin stabilization of attitude against gravity torque," J. Astronaut. Sci. **IX**, 31–33 (Spring 1962).

[3] Kane, T. R., Discussion and correction of stability curve presented in Ref. 2, J. Astronaut. Sci. **IX**, 108–109 (1962).

[4] Cunningham, W. J., *Introduction to Nonlinear Analysis* (McGraw-Hill Book Co. Inc., New York, 1958), pp. 270–274.

JULY 1963 AIAA JOURNAL VOL. 1, NO. 7

Design of Lunar and Interplanetary Ascent Trajectories

VICTOR C. CLARKE JR.*

Jet Propulsion Laboratory, California Institute of Technology, Pasadena, Calif.

The near-Earth or "ascent" portion of lunar and interplanetary trajectories is investigated. Of particular interest is the matching of the powered-flight and coasting phases. To achieve a suitable match, consideration of vehicle-related engineering constraints, payload, and geometrical and energy requirements imposed by the extraterrestrial trajectory is essential. The geometrical constraints and trajectory shaping are treated in detail. To satisfy these constraints, direct-ascent and parking-orbit types of trajectories are investigated and compared. Advantages and disadvantages of each are noted. The superiority of the parking-orbit type is illustrated. It is shown that this type has consistently greater payload capability and provides a convenient method of launch-time delay compensation. Finally, injection locations of Mars and Venus trajectories using parking orbits are mapped.

I. Introduction

THE initial phases of lunar and interplanetary trajectories possess certain common properties that permit a unified analytical treatment of both at the same time. These common properties are primarily geometrical in nature. In this paper, the chief consideration is that phase of flight from launch until the time when the spacecraft is essentially traveling radially outward from the Earth. This phase of flight is termed the "ascent" phase. As will be seen, the design of the ascent trajectory is influenced heavily by several factors.

For purposes of obtaining a gross understanding of ascent trajectory design, it is worthwhile to assume the two-body approximation that the near-Earth path of a lunar trajectory is an ellipse or a hyperbola and the near-Earth path of an interplanetary trajectory is a hyperbola. In actual practice, of course, perturbative effects of Earth's oblateness and celestial bodies, as needed, must be included.

The chief problem of ascent trajectory design is that of matching the powered portions of flight to the final coasting portion. The interaction of these two portions of flight is quite strong. For example, an infinite number of physically realizable ascent trajectories will produce overall lunar or interplanetary flights that satisfy the mission requirement. However, only a small set of these is suitable from a practical standpoint. The practicality of a set of trajectories must be based on engineering considerations such as payload weight, guidance, tracking and telemetry, reliability, vehicle-related constraints, etc. Thus, engineering considerations strongly determine the ascent trajectory in conjunction with the requirements of the overall trajectory.

It is the purpose of this paper to examine the characteristics of lunar and interplanetary ascent trajectories and the factors that determine them. Chief among these factors are the powered-flight phases and the geometrical constraints imposed by the overall trajectory. The geometrical constraints will be considered first.

Received by IAS July 5, 1962; revision received December 28, 1962. This paper presents the results of one phase of research carried out at the Jet Propulsion Laboratory, California Institute of Technology, under Contract NAS7-100, sponsored by NASA.

* Engineering Group Supervisor.

II. Geometrical Properties

Three geometrical properties that strongly influence the ascent trajectory are launch site location, the outward radial direction, and launch azimuth.

A. Launch Location

The first property, launch site location, is an independent variable of the geometry problem which is not changed easily because of the great cost and logistic, communication, and political problems involved. Thus, for firings from the United States, it is logical to assume the launch facility at Cape Canaveral, Atlantic Missile Range (AMR) for our purposes. Lunar and interplanetary launchings from the launch facility of the Pacific Missile Range (PMR) are unde-

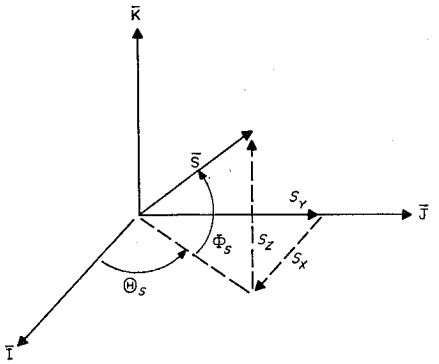

Fig. 1 Geometry of the outward radial direction

sirable for two reasons: 1) payload losses are incurred by the presumed restriction to southerly or westward launchings; and 2) for southerly launchings, the launch-on-time problem is severe. Construction of an equatorial launch site for lunar and interplanetary missions can be shown to be completely unnecessary, especially through use of the parking orbit (to be discussed below).

B. Outward Radial Direction

The second geometrical constraint, the outward radial direction, has the strongest influence on the ascent trajectory. For slow (elliptical motion) lunar trajectories, the outward radial direction is defined to be the direction from Earth to moon at encounter. For fast (hyperbolic motion) lunar and interplanetary trajectories, the outward radial direction is defined to be the direction of the outgoing asymptote of the escape hyperbola. The assumption here is that a lunar trajectory can be approximated closely by a single Earth conic. A better approximation, of course, is two patched conics, one relative to the Earth and one relative to the moon. However, it has been perceived that the one conic approximation is sufficiently valid for the stated purposes here, i.e., to achieve a gross understanding of ascent trajectory design. The approximation of one hyperbolic conic section near the Earth (less than 500,000 miles) for interplanetary trajectories is adequate for our purpose also.

Let the outward radial direction be represented by a unit vector **S** in an X-Y-Z Cartesian frame, where positive X is in the direction of the vernal equinox, positive Z is in the direction of the Earth spinvector, and positive Y is in right-handed relation to X and Z. Thus X and Y lie in the Earth's equatorial plane. A position vector **R** from Earth center to a spacecraft is defined as

$$\mathbf{R} = \mathbf{I}X + \mathbf{J}Y + \mathbf{K}Z \tag{1}$$

where **I**,**J**,**K** are unit vectors in the X,Y,Z directions, respectively. The unit vector **S** could be expressed alternately as

$$\mathbf{S} = \mathbf{I}S_X + \mathbf{J}S_Y + \mathbf{K}S_Z \tag{2}$$

or

$$\mathbf{S} = \mathbf{I}\cos\Theta_S\cos\Phi_S + \mathbf{J}\sin\Theta_S\cos\Phi_S + \mathbf{K}\sin\Phi_S \tag{3}$$

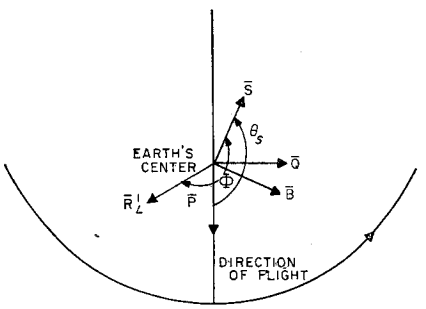

Fig. 2 Trajectory-plane geometry

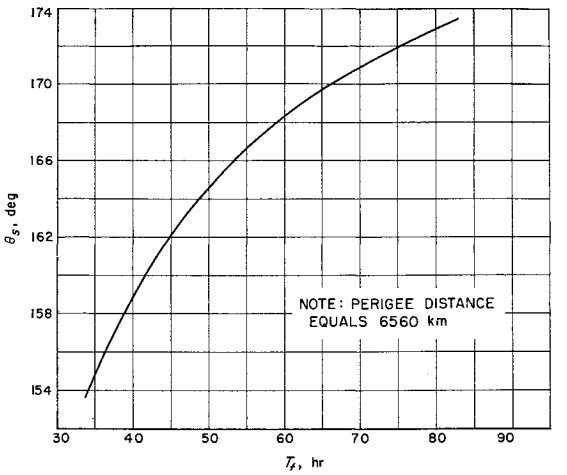

Fig. 3 Angle between outward radial and perigee vs lunar flight time

where Θ_S and Φ_S are the right ascension and declination of **S**, respectively (see Fig. 1).

By specifying the launch date and flight time of the mission, the outward radial **S** as well as the energy† C_3 of the near-Earth conic become known quantities. This follows from the fact that the four defining quantities of a lunar or interplanetary trajectory are launch date, right ascension and declination of the outward radial, and the energy C_3. Other sets of quantities may be used to define a trajectory; however, this set of four is minimal and most convenient.

Assume that the overall mission is specified; then **S** and energy C_3 are constants of the problem. Thus, it follows that the final criterion for ascent trajectory design is simply that it satisfy the four parameters. At least two requirements immediately become apparent: 1) thrust must be applied until the required energy is achieved; and 2) the trajectory plane must contain the outward radial **S**. The second requirement is most interesting because it is the root of the geometry problem. This problem will be treated now in detail.

Consider the geometry of Fig. 2. Here is shown a portion of the near-Earth conic (either an ellipse or hyperbola). The plane of motion is in the plane of the page. A unit vector **W** (not shown), perpendicular to the plane (up out of the page), defines the plane. The unit vector **P** is directed toward perigee, and **Q** is in right-handed relation to **W** and **P** such that $\mathbf{Q} = \mathbf{W} \times \mathbf{P}$.

The vectors **P** and **Q** are determined by **S** and **W** as follows:

$$\mathbf{P} = \mathbf{S}\cos\theta_S + \mathbf{B}\sin\theta_S \tag{4}$$

$$\mathbf{Q} = \mathbf{S}\sin\theta_S - \mathbf{B}\cos\theta_S \tag{5}$$

Here $\mathbf{B} = \mathbf{S} \times \mathbf{W}$, and θ_S is the angle subtended between perigee and the outward radial direction. This angle is determined for hyperbolic conics from the formula

$$\cos\theta_S = -(1/e) \qquad 0 \leq \theta_S \leq \pi \tag{6}$$

where e is the eccentricity of the hyperbola.

For elliptical conics,

$$\cos\theta_S = (p - R_I)/eR_I \qquad 0 \leq \theta_S \leq \pi \tag{7}$$

where p is the semilatus recum, and R_I is the magnitude of the Earth-to-moon position vector at encounter time.

The outward radial central angle θ_S is an important quantity in determining the ascent trajectory also. This angle will vary depending on the mission. For lunar missions, it is heavily dependent on the chosen flight time (or injection

† The energy C_3 is actually twice the energy per unit mass, i.e., the vis viva integral, $V^2 = C_3 + (2GM/R)$, where R is the injection radius and V is the injection speed.

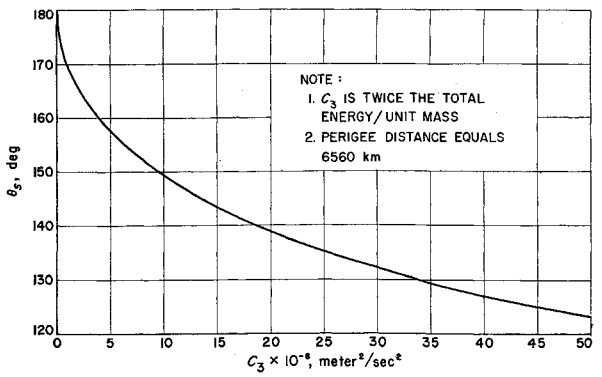

Fig. 4 Angle between outward radial (asymptote) and perigee as a function of energy C_3 for interplanetary trajectories

energy). For lunar flight times of 30 to 90 hr, θ_S will vary from 150° to 175°, as shown in Fig. 3. For a 66-hr trajectory, the angle will be about 170°.

For interplanetary missions, the values of θ_S range from about 125° to 155°, a decrease relative to the lunar case. The decrease of θ_S with increasing injection energy C_3 is illustrated in Fig. 4. Injection energy strongly determines flight time to the planet. Typically, an energy $C_3 = 0.2 \times 10^8$ m^2/sec^2 will provide a trip of 177 days to Mars if it were launched on November 5, 1962. The outward radial direction angle θ_S will be 139° in this case.

The central angle θ_S is important because it determines where perigee is located relative to the known outward radial direction **S** in the trajectory plane.

The in-plane relations being established, the orientation of the trajectory plane in the X-Y-Z system will be considered now. To do this, note that

$$\mathbf{W}\cdot\mathbf{S} = 0 \tag{8}$$

$$\mathbf{W}\cdot\mathbf{W} = 1 \tag{9}$$

Equations (8) and (9) can be solved simultaneously to yield

$$W_Y = \frac{-W_Z S_Y S_Z \pm S_X(1 - S_Z^2 - W_Z^2)^{1/2}}{S_X^2 + S_Y^2} \tag{10}$$

$$W_X = \frac{-[W_Y S_Y + W_Z S_Z]}{S_X} \tag{11}$$

Equations (10) and (11) giving the X and Y components of **W** are solved in terms of the known components of **S** and in terms of the component W_Z. The reason W_Z is chosen as an independent variable is that W_Z is a function of the planar inclination or launch azimuth only. The component W_Z is related to inclination and launch azimuth by the formula

$$W_Z = \cos i = \cos\Phi_L \sin\Sigma_L \tag{12}$$

where i is the orbital-equatorial plane inclination angle, Φ_L is the launch site declination, and Σ_L is the launch azimuth measured positive east of true north (see Fig. 5).

From Eqs. (10–12), it can be seen that, given a launch site, choice of launch azimuth determines not one, but two space-fixed planes of motion because of the plus-minus signs in Eq. (10). Since the planes are space-fixed and the launch site is rotating in space, the launch site may pass through each plane twice each day. What this means is that there could be two launch times per day for a given launch azimuth, or once for each plane. Referring back to Eq. (10), it is noted that there are launch azimuths at which it is not possible to fire. This occurs when

$$W_Z^2 > 1 - S_Z^2 \tag{13}$$

or

$$\sin^2\Sigma_L > \cos^2\Phi_S/\cos^2\Phi_L \tag{14}$$

since $S_Z = \sin\Phi_S$. Limiting or boundary values of launch azimuth exist where firing is marginally possible.

The limiting cases are when

$$W_Z^2 = 1 - S_Z^2 \tag{15}$$

or

$$\sin\Sigma_L = \pm\cos\Phi_S/\cos\Phi_L \tag{16}$$

and since

$$-(\pi/2) \leq \Phi_S \leq \pi/2$$

and

$$-(\pi/2) \leq \Phi_L \leq \pi/2$$

then two values‡ of Σ_L are obtainable in the first and second quadrants. These values correspond to limiting northeast and southeast launch azimuths. If Σ_{LI} is the limiting northeast azimuth and Σ_{LII} is the limiting southeast azimuth, then no firings are possible for $\Sigma_{LI} < \Sigma_L < \Sigma_{LII}$. For example, if the declination (Φ_S) of the outward radial is 45° and the launch site latitude is 28.4°, then for launch azimuths between 53.5° and 126.5° no firings are possible.

Generally, if the declination of the outward radial is greater than the launch site latitude, a range of launch azimuths (symmetrical about due east) exists at which it is not possible to fire from that site. If the outward radial declination is less than or equal to the launch site latitude, it is possible to fire at all launch azimuths within range-safety limits.

The point of view which has been taken here is that the orientation of the trajectory plane is determined by rotating the plane about the outward radial direction **S** to a set value of inclination and then waiting until the launcher passes through the plane before firing. Another point of view can be taken, as described below.

C. Further Effect of Launch Azimuth

The effect of launch azimuth on the geometry problem is that it determines the inclination of the trajectory plane relative to the equatorial plane. When launch azimuth is varied, the trajectory plane is rotated about a line joining the Earth's

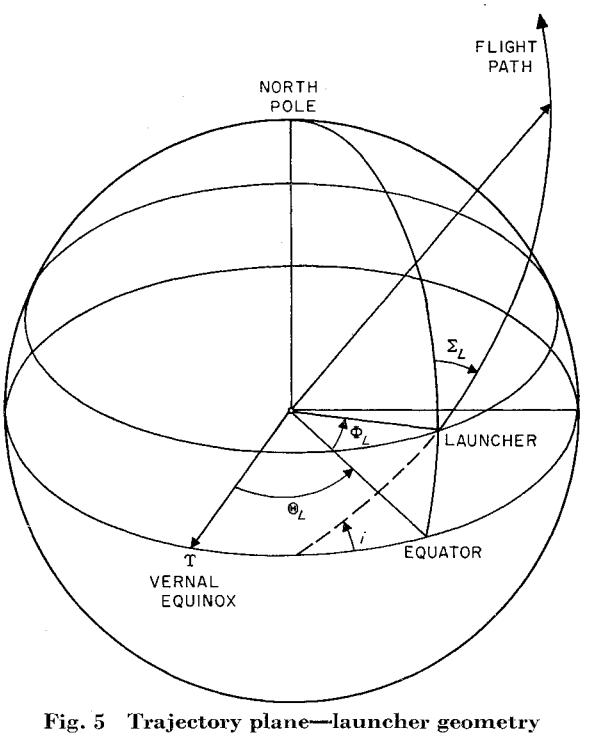

Fig. 5 Trajectory plane—launcher geometry

‡ Westerly firings from Cape Canaveral are not considered.

center and the launch site. However, this rotation can take place only under certain restrictions. Recall that it was stated that the trajectory plane must contain the outward radial **S**. Thus, the trajectory plane must contain both the launcher at launch time and the vector **S**. If launch time is prespecified, the launch azimuth must be chosen such that the trajectory plane contains **S**. On the other hand, if the launch azimuth is fixed, launch must occur at the proper time.

Herein lies the difference in the two points of view in the geometry problem. In the first case, it was considered that the trajectory plane contains **S** and was fixed in space at a specified inclination to the equatorial plane. Launch then must occur when the launch site passes through the space-fixed plane. In the second case, it is considered that the trajectory plane contains the launch site and is rotating in space. Launch occurs at the instant the plane passes through the outward radial **S**. Both points of view are useful in visualizing the problem. No matter what point of view is taken, it is evident that there is a strong relationship between launch time and launch azimuth. Furthermore, it is apparent that there is a problem of launching at the proper time, given a certain launch azimuth. This problem is commonly known as the launch-on-time problem. Since there is a strong relation between launch azimuth and launch time, it also should be apparent that this relationship can form the basis for solution of the launch-on-time problem, as it does, of course.

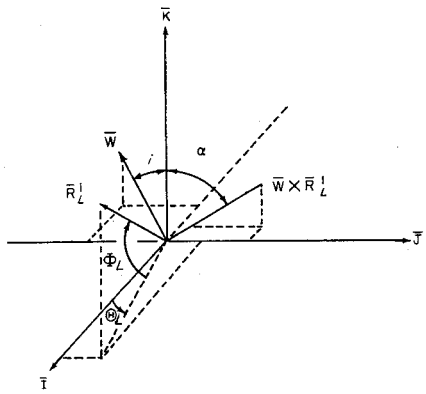

Fig. 6 Launch site geometry

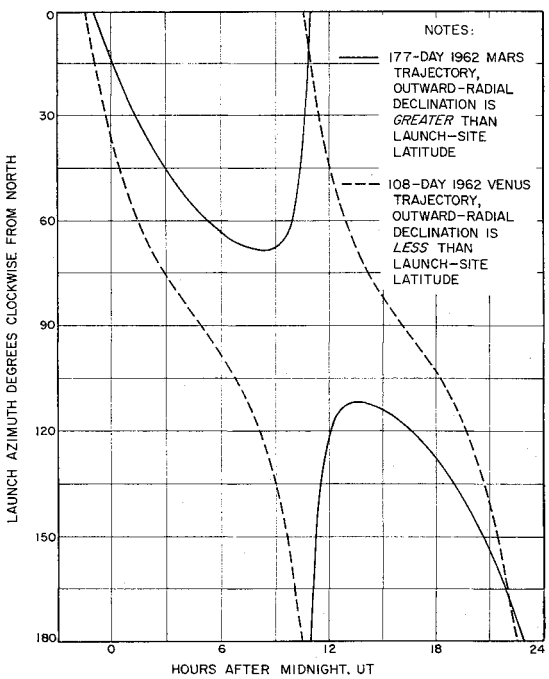

Fig. 7 Example of launch azimuth vs launch time

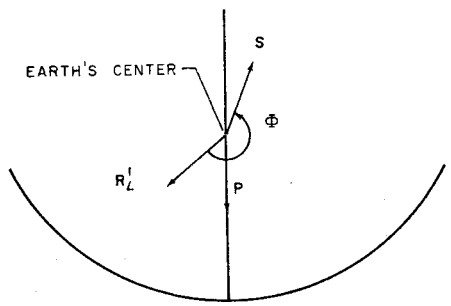

Fig. 8 Launcher-outward radial central angle

D. Launch Time

To determine the relationship between launch time and launch azimuth, note that, when the launch site passes through the space-fixed trajectory plane, these relations must hold (see Fig. 6):

$$\mathbf{R}_L{}^1 \cdot \mathbf{W} = 0 \tag{17}$$

$$(\mathbf{W} \times \mathbf{R}_L{}^1) \cdot \mathbf{K} = \cos\alpha = (\cos^2\Phi_L - W_Z{}^2)^{1/2} \tag{18}$$

where $\mathbf{R}_L{}^1$ is a unit vector directed from the Earth's center to the launch site given by

$$\mathbf{R}_L{}^1 = \mathbf{I}\cos\Theta_L \cos\Phi_L + \mathbf{J}\sin\Theta_L \cos\Phi_L + \mathbf{K}\sin\Phi_L \tag{19}$$

where Φ_L is the launch site declination, and Θ_L is the right ascension of the launch site and is related to time by

$$\Theta_L = GHA + \theta_L + \omega t_L \tag{20}$$

where GHA is the Greenwich Hour Angle at midnight of the launch day, θ_L is the longitude of the launch site, ω is the angular speed of the earth, and t_L is the time from midnight on the launch day.

Equations (17) and (18) can be solved simultaneously to find the launcher right ascension, and hence the launch time:

$$\cos\Theta_L = \frac{W_Z W_X \sin\Phi_L + W_Y(\cos^2\Phi_L - W_Z{}^2)^{1/2}}{(W_Z{}^2 - 1)\cos\Phi_L} \tag{21}$$

$$\sin\Theta_L = \frac{W_Y W_Z \sin\Phi_L - W_X(\cos^2\Phi_L - W_Z{}^2)^{1/2}}{(W_Z{}^2 - 1)\cos\Phi_L} \tag{22}$$

Components W_X, W_Y, and W_Z are all functions of launch azimuth and the components of the outward radial **S**. Therefore, the time of launch is determined solely (given the launch site) by launch azimuth and by the right ascension and declination of the outward radial **S**.

An example of plots of launch azimuth vs launch time for two declinations of the outward radial is shown in Fig. 7. It should be noted that the time rate-of-change of launch

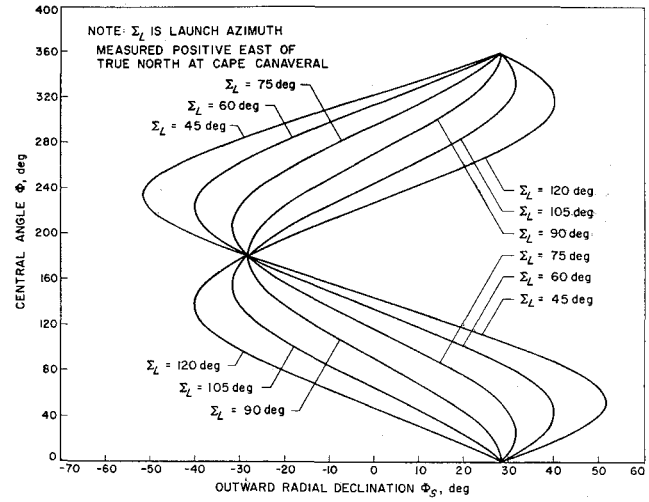

Fig. 9 Angle between launch and outward radial vs outward radial declination

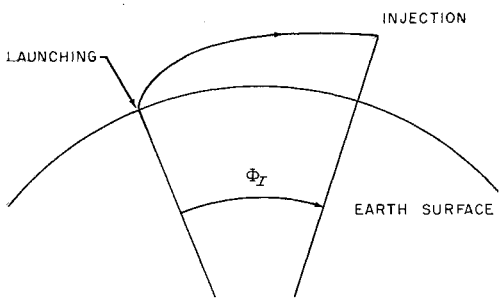

Fig. 10 Altitude-range profile

azimuth goes through zero in the case where the declination of the outward radial is greater than the launch site latitude. When this derivative is zero, it is the best time to fire. In the plots of Fig. 7, the independent variable has been switched from launch azimuth to launch time. Other plots interchanging the variables also are useful.

E. Launcher-Outward Radial Central Angle

As previously stated, launch occurs when both the outward radial **S** and the launch site are contained in the trajectory plane. An important quantity in the geometry problem is the magnitude of the launcher-to-outward radial central angle Φ, shown in Fig. 8.

Basically, the central angle Φ is the total angle that the vehicle must sweep out from launch until it is a large distance from the Earth. Given a launch site, this angle depends chiefly on two quantities: launch azimuth and declination of the outward radial. In addition, it is double-valued, corresponding to the two possible launch times each day for a specified launch azimuth. Plots of Φ as a function of outward radial declination are shown in Fig. 9. Launch azimuth is a parameter in both cases.

F. Geometry Problem Summary

Thus far, certain geometrical aspects of lunar and interplanetary trajectories have been examined. It is wise to pause briefly to summarize before discussing the matching of the powered-flight phase to the geometrical constraints. Several factors have been determined: 1) the launch site location is relatively invariant: Cape Canaveral logically has been chosen; 2) when the overall mission is specified, the outward radial direction **S** and injection energy are specified automatically; 3) the perigee location is determined from **S** and the central angle θ_S between the outward radial and perigee; the angle θ_S is determined basically by injection energy; 4) for an assumed launch azimuth, two launch times may be possible each day (or vice versa; if a launch time is assumed, launch azimuth is determined); also, depending on the relationship of launch-site latitude and the declination of the outward radial, no launches may be possible for a symmetrical band of launch azimuths about due east; and 5) since the trajectory plane must contain both the launcher and outward radial, there is a certain central angle Φ between **S** and the launcher which the vehicle *must* traverse in going from launch to a large distance from Earth.

With these points in mind, properties of the powered phases may be discussed, and the powered phases subsequently may be matched to the geometrical constraints.

III. Powered-Flight Phases

A. General

A general discussion of the powered-flight phases of lunar and interplanetary trajectories is somewhat difficult because their characteristics are strongly vehicle-dependent. In particular, the acceleration-time profile of each vehicle stage heavily determines the altitude-range profile.

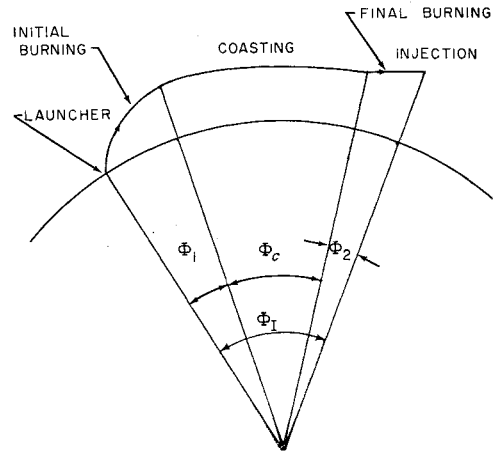

Fig. 11 Powered trajectory modified by coasting

A characteristic of interest is the arc Φ_I subtended at Earth's center in the trajectory plane during burning as shown in Fig. 10. The burning arc Φ_I will vary depending on the vehicle's acceleration-time profile and the injection energy. Associated with the arc Φ_I will be a burning time t_I. It is assumed that, in traversing the arc Φ_I, the thrust vector direction is programmed in a manner that tends to maximize payload while still satisfying any vehicle-related engineering constraints.

It is conceivable that the required injection energy may be achieved by one of two methods. The first and most obvious method would be to burn the stages successively and continuously, allowing only short coasts (or small ullage propulsion phases) between stages to accomplish the staging separation sequences successfully. The second method is to break up the burning phase into three separate arcs, as shown in Fig. 11.

Here, in an initial burning phase the vehicle sweeps out an arc Φ_1 in time t_1 and then coasts over an arc Φ_c for time t_c. A final burning phase for time t_2 terminates in injection into an elliptical or hyperbolic conic.

Method one, employing continuous, successive burning stages, hereafter will be termed a "direct-ascent" trajectory. Method two, employing a circular coasting interval between stages, hereafter will be termed a "parking-orbit" trajectory. Both types of powered-ascent phases can be used for lunar and interplanetary trajectories. Both have certain advantages and disadvantages. However, as will be shown, the parking-orbit type offers far greater flexibility in meeting the geometrical constraints. The characteristics of each type now will be examined and the advantages and disadvantages of each weighed.

B. Direct-Ascent Trajectories

At the end of the powered phase, the vehicle not only must have the required injection energy but also must inject into an orbit that satisfies the geometrical constraints. Herein lies a major disadvantage of the direct-ascent trajectory. The two objectives of satisfying energy requirements and geometrical constraints simultaneously with direct-ascent trajectories can be met only very seldom, and then only under a rather restricted set of conditions. The basic reason for this is that in order to satisfy the geometrical constraints it usually is necessary to use a highly inefficient powered path resulting in large payload losses, even to the point where there is no payload left at all. Specifically, in order to satisfy the geometrical constraints, it is necessary to fly steeper trajectories. Steep trajectories are less efficient than flat ones because of greater velocity loss due to gravitational effects over the burning interval. To illustrate this inefficiency, Fig. 12 shows per-

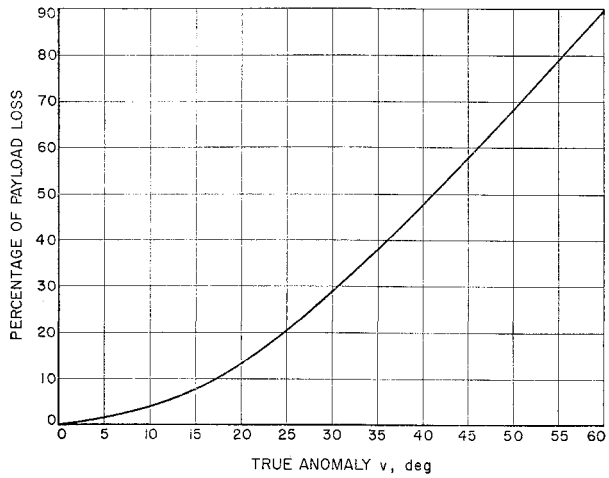

Fig. 12 Percentage of payload loss vs true anomaly

centage payload loss as a function of true anomaly at injection. The true anomaly $\hat{\theta}$ is the angle subtended at Earth's center between perigee and injection. It generally is found that the most efficient (payloadwise) point of injection is near perigee. The reason it is necessary to fly steep, inefficient trajectories is that they provide large values of true anomaly. These large values are necessary to satisfy the required launcher-outward radial central angle Φ. To illustrate this, consider Fig. 13 in the plane of the conic.

Here $\mathbf{R}_L$ is the position vector of the launch site, and $\mathbf{R}$ is the position vector at injection. From Fig. 13, one can write an important relation:

$$\hat{\theta} = \theta_S - \Phi + \Phi_I \tag{23}$$

which says the required true anomaly $\hat{\theta}$ is a function of the perigee-outward radial angle θ_S, the launch-outward radial angle Φ, and the burning arc Φ_I. As discussed previously, θ_S and Φ are functions of the mission. The burning arc Φ_I usually lies in the range from 15° to 45°, depending on the vehicle and injection energy. Given a mission, the value of true anomaly is determined. Thus, a definite relationship is established between mission requirements and payload via the true anomaly. Unless the right-hand side of Eq. (23) adds up to about zero, payload loss results. In the majority of cases, $\hat{\theta}$ does not fall near zero, and the mission must be reselected carefully (or abandoned) so that it does. Before altering the mission, however, the design process requires that an attempt be made to juggle the right-hand side of Eq. (23) so that $\hat{\theta}$ falls near perigee range. The quantities θ_S and Φ_I are relatively invariant, because both the size and shape of the post-injection conic are determined strongly by the injection energy C_3. That is, the eccentricity and angular momentum of the conic are determined basically by injection energy. This is true irrespective of the shape of the powered path. Thus, only the launcher-outward radial angle Φ can be varied to any extent by changing launch azimuth (refer back to Fig. 9). If variation of a launch azimuth (within range-safety limits) does not improve payload sufficiently by changing the required true anomaly, then the mission must be reselected.

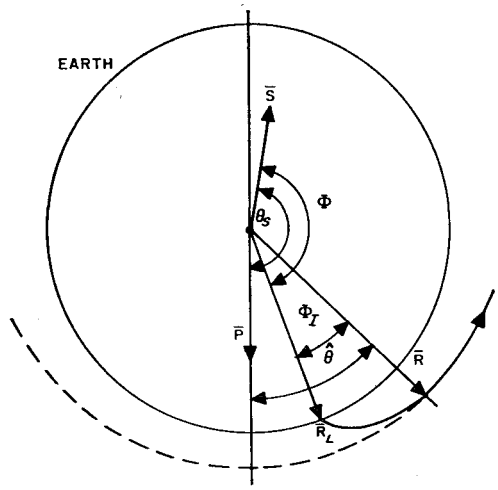

Fig. 13 Ascent trajectory geometry

A very important quantity in deciding whether direct-ascent powered trajectories are feasible is the declination of the outward radial **S**. This quantity is determined by mission requirements and strongly determines the launcher-outward radial angle Φ (again refer to Fig. 9). Generally, it is found that a combination of northeast launch azimuths and negative values (less than −15°) of outward radial declination results in feasible direct-ascent trajectories. Although they may be feasible, they would, in most cases, have less payload capability than parking-orbit type trajectories.

In addition to having poor payload capability, the launch-on-time problem is more severe for direct-ascent than for parking-orbit type trajectories. The firing windows each day are much smaller, and the variation of launch azimuth with launch time is greater. No validating arguments will be advanced here on this point. The launch-on-time problem is a study in itself. Another disadvantage of the direct-ascent trajectory is that, since northeast azimuths must be used, a danger exists that the boost stages may fall on the European continent.

A few advantages of direct-ascent powered trajectories may be mentioned. One is the preinjection tracking and telemetry coverage possibilities. Since all burning occurs near the launch site and the trajectory is steeper, visibility from existing range instrumentation possibly may be enhanced. Since northeast azimuths must be used, stations at Bermuda and on the east coast of the United States and Canada may be used.

Perhaps the greatest advantage is the fact that engineering problems of attitude control and other aspects of vehicle engineering are reduced by direct-ascent trajectories. No long coast periods are encountered. Dissipation of cryogenic propellants (if used) is minimized, and a restart capability of the last-stage engine is unnecessary.

In summary, it appears that the disadvantages of direct-ascent powered trajectories far outweigh their advantages. Undoubtedly, other favorable arguments could be advanced in their behalf. But, on the other hand, they could be degraded further also. Parking-orbit trajectories will be dis-

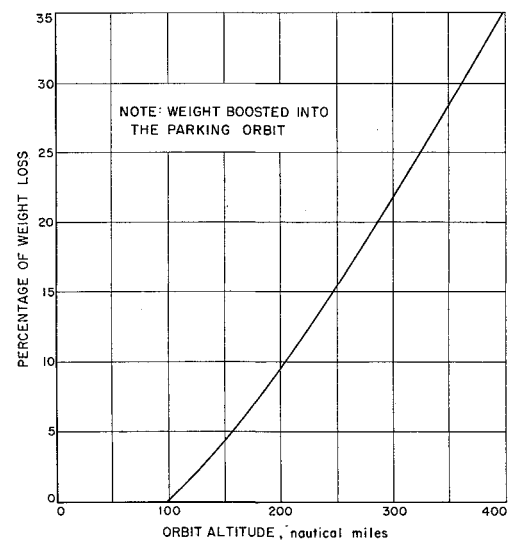

Fig. 14 Percentage of weight loss as a function of parking-orbit altitude

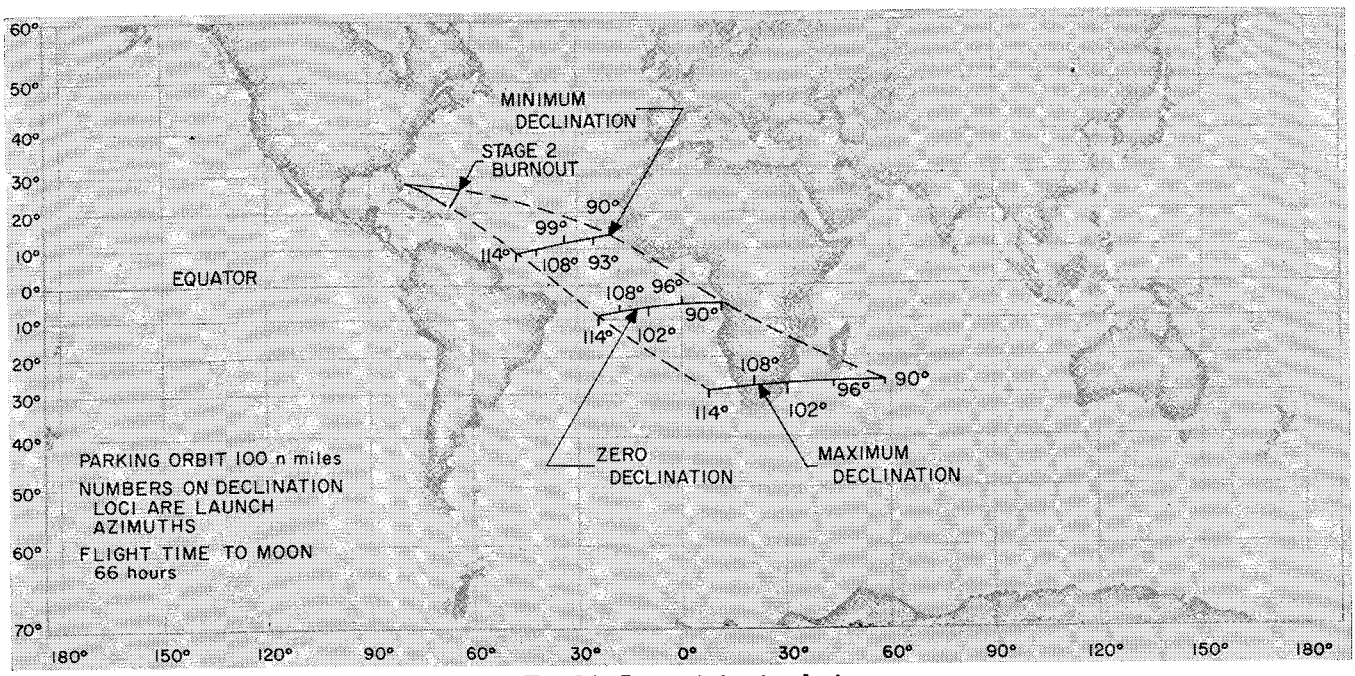

Fig. 15 Lunar injection loci

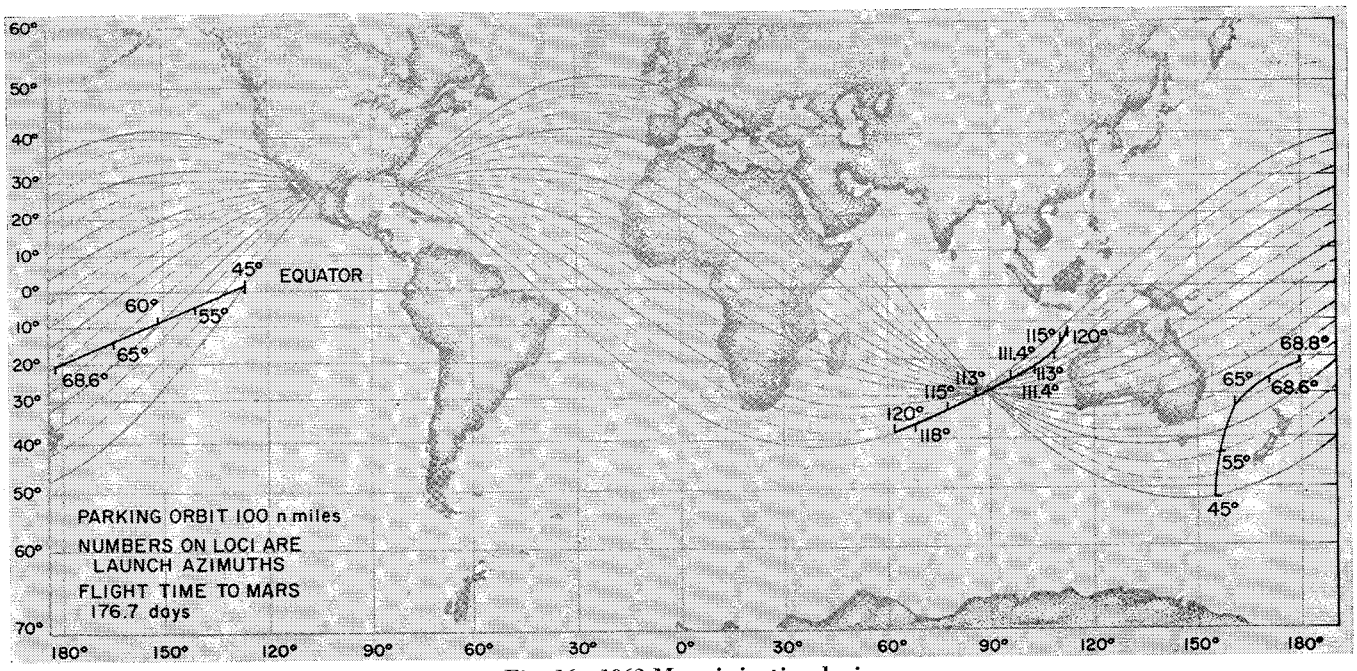

Fig. 16 1962 Mars injection loci

cussed now, and it will be shown how they alleviate the major problems of the direct-ascent type.

C. Parking-Orbit§ Trajectories

The introduction of an intermediate circular coast (Fig. 11), or parking orbit, into the powered-flight phase greatly facilitates handling of the geometrical constraints while still providing good payload capability. Reconsider Eq. (23), and recall that, in order to provide good payload capability, the true anomaly $\hat{\theta}$ should be near perigee, i.e., $\hat{\theta}$ approximately 0°. Since θ_S and Φ_I are relatively invariant, it is necessary to make $\hat{\theta}$ fall in this range by varying the launcher-outward radial central angle Φ. To vary Φ, launch azimuth and/or the outward radial declination must be changed. Launch azimuth variation is restricted by range-safety limits. To change the outward radial declination, the mission must be altered. At best, the central angle Φ is a rather "restricted" variable with definite limits. To overcome these restrictions, the new "unrestricted" independent variable is introduced. This variable is the coasting arc Φ_c, which is contained in the total burning arc Φ_I by

$$\Phi_I = \Phi_1 + \Phi_c + \Phi_2 \tag{24}$$

Here again Φ_1 is the burning arc necessary to get into the parking orbit, and Φ_2 is the burning arc from parking orbit to final injection.

The introduction of the variable coast arc Φ_c removes the relative invariance of the total burning arc Φ_1 and allows great flexibility to satisfy the geometrical constraints. Theoretically, the coasting arc may have any value from zero to infinity; however, coasting up to one revolution around the Earth is sufficient to solve the problem. With the flexibility provided by coasting, launch azimuth may be chosen at will and

§ To the author's knowledge, the parking orbit first was suggested by Krafft A. Ehricke.

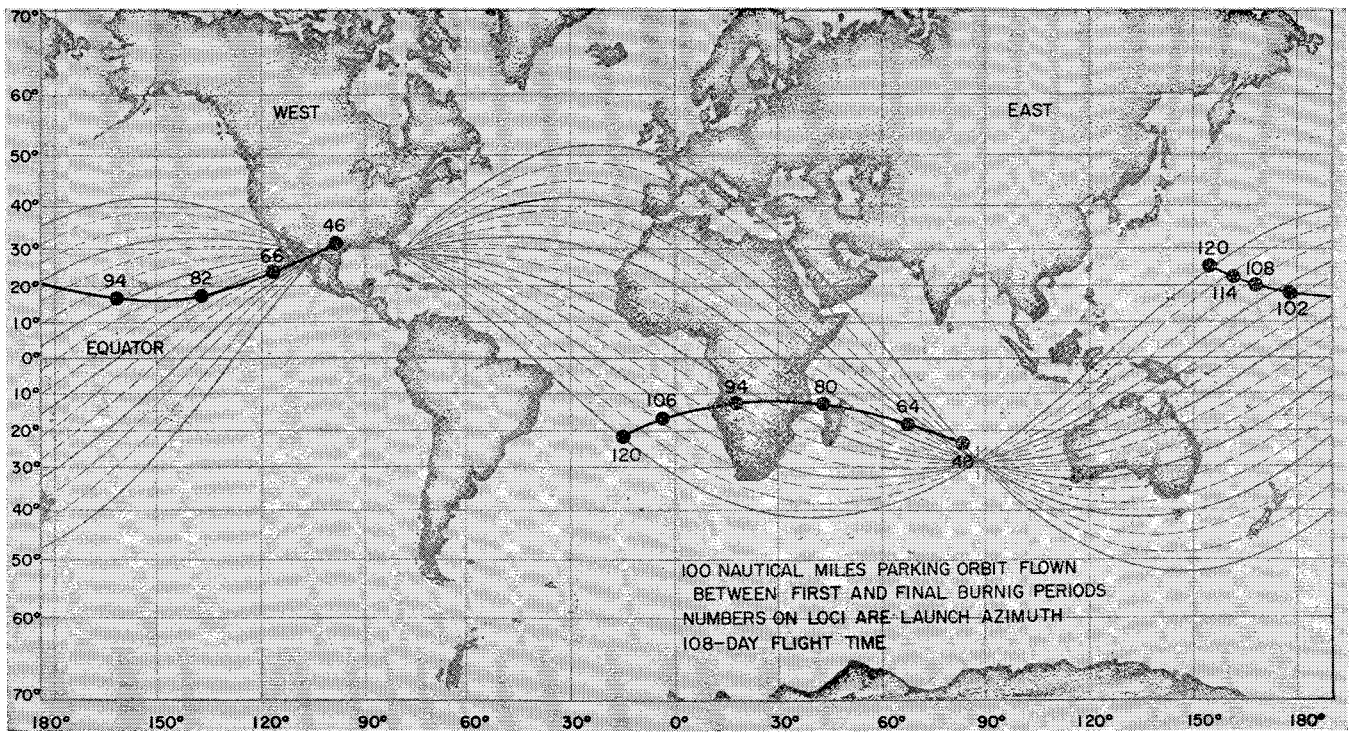

Fig. 17 1962 Venus injection loci

the mission left unaltered, since there is no need to vary outward-radial declination. Given a launch azimuth and mission, the matching of the powered-flight phase to the postinjection trajectory is completed by varying launch time and parking-orbit coast time. Or given a launch time and mission, launch azimuth and parking-orbit coast time may be varied to match the powered phase to the postinjection trajectory. Herein lies the final step in solving the launch-on-time problem also. By simultaneous variation of launch azimuth and coast time in the parking orbit, it is theoretically possible to fire at *any time of the day.* Practically, of course, it is not possible to fire at any time because of range-safety limits. Even if range safety were disregarded, it would be undesirable to shoot at near due north or due south azimuths because the rate-of-change of launch azimuth with launch time tends to infinity in those cases.

Thus, two major advantages of parking orbits have been seen: 1) the ease of solving the geometry problem, and 2) a simple solution of the launch-on-time problem. A third advantage is good payload capability. By using a low-altitude parking orbit, a relatively flat powered trajectory can be employed.

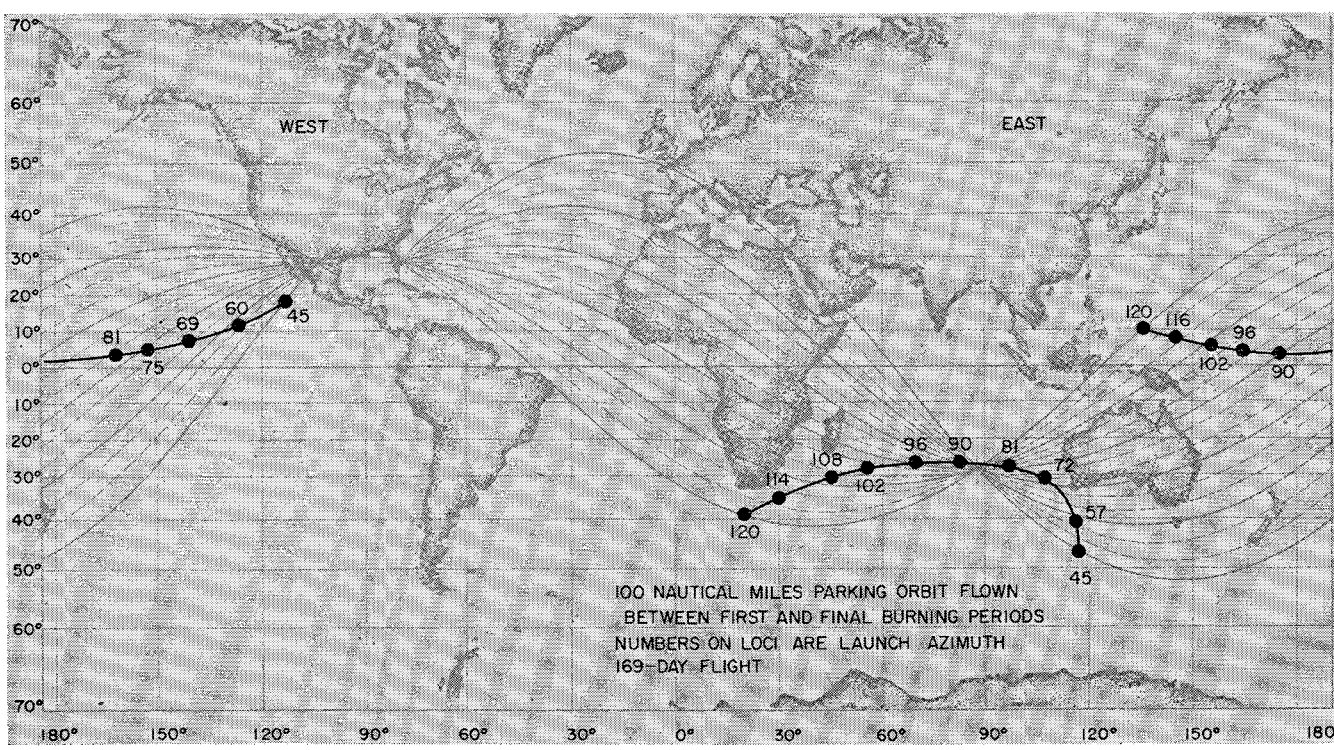

Fig. 18 1964 Mars injection loci

In choosing the altitude of the parking orbit, the lowest possible value yields greatest payloads. The minimum altitude depends on vehicle-related engineering constraints such as aerodynamic heating and structural loading. Furthermore, additional limitations are imposed if a radio guidance system is used during the initial burning phase. The radar elevation angle must be held above a certain minimum value; otherwise, accuracy is degraded.

The practical minimum parking-orbit altitude is near the range of 80 to 110 naut miles. Weight into the parking orbit diminishes as its altitude is increased, as shown in Fig. 14. In this figure, weight is normalized to the 100-naut-mile parking-orbit altitude. After coasting in the parking orbit for the specified time, injection energy is achieved by a final burning phase. Injection occurs 3° to 10° past perigee, depending on the vehicle and injection energy. It has been perceived that the parking-orbit altitude and the perigee of the postinjection conic are extremely close in value—as close as 1 km. This fact is very useful in closely estimating the shape of the postinjection conic, since the eccentricity is given by

$$e = 1 + (R_p C_3/GM_E) \tag{25}$$

where R_p is the perigee distance from Earth's center of the postinjection conic, G is the universal gravitational constant, and M_E is the mass of the Earth. Since the energy C_3 is known and the perigee altitude distance essentially is equivalent to parking-orbit altitude, the eccentricity may be found from Eq. (25). This determines the conic's shape. Since energy and eccentricity are known, the angular momentum C_1 thereby may be found.

Some disadvantages of parking orbits may be mentioned also. Probably the most serious is the preinjection tracking and telemetry coverage problem. Not only is the altitude low, but the location of the final burning phase will vary considerably with launch time delay. Because of the need for a low (100-naut-mile) parking-orbit altitude, the region of visibility from tracking/telemetry stations is reduced. Location of the final burning phase will vary from minute to minute during a given launch day in addition to varying from day to day. The reason the location varies from minute to minute during the day is that, in compensating for launch-time delay, the launch-azimuth and parking-orbit coast time must be varied, resulting in a shift of the injection point. The injection location can be found from the following relations:

$$\mathbf{R}^1 = \mathbf{P}\cos\hat{\theta} + \mathbf{Q}\sin\hat{\theta} \tag{26}$$

where $\mathbf{R}^1$ is a unit vector directed from Earth's center to injection given by

$$\mathbf{R}^1 = \mathbf{I}\cos\Theta_I\cos\Phi_I + \mathbf{J}\sin\Theta_I\cos\Phi_I + \mathbf{K}\sin\Phi_I \tag{27}$$

Here Θ_I is the right ascension of injection, and Φ_I is the injection declination. The longitude of injection may be found by

$$\theta_I = \Theta_I - \Theta_L - \omega t_I + \theta_L \tag{28}$$

where Θ_L is the launcher right ascension, and θ_L is the launcher longitude. The time from launch to injection, t_I, may be determined from

$$t_I = t_1 + t_2 + k\Phi_c \tag{29}$$

where $k = 1/\dot{\Phi}_c$ = constant parking orbital rate in seconds per degree, equal to 14.678 sec/deg for a 100-naut-mile parking orbit.

An illustration of how injection location can vary during the lunar month is shown in Fig. 15. Injection can fall anywhere within the dotted area in the Atlantic Ocean, depending on the launch day during the month and the launch time during the day. Launch azimuths were restricted arbitrarily here to the range of 90° to 114°. Another injection region also can be found in the Pacific area for this range of azimuths. This second region corresponds to the second permissible launch time per launch azimuth per day. These cases require considerably longer parking orbits and may be rejected tentatively on engineering grounds. Loci of injection points for a 177-day Mars and 108-day Venus trajectories in 1962 are shown in Figs. 16 and 17. Note that in the Mars case no launch is permitted between 68.716° and 111.284°. In this case, the declination of the outward radial is greater than the launch site latitude; hence, the limitation on launch azimuth is present, as explained earlier. However, in 1964 the Mars location situation changes, as shown in Fig. 18. Here the declination of the outward radial is less than the launch-site latitude.

A second disadvantage of parking orbits is that the last stage must have a restart capability. This implies ullage problems. Guidance accuracy at parking-orbit injection must be such that the probe does not dip down into the atmosphere on long coasts. Cryogenic propellants will be lost during long coasts. In general, parking orbits present a set of particular engineering problems.

IV. Conclusion

In this paper, the author has endeavored to point out some of the facets of ascent trajectory design. In particular, the problematical relationship between geometrical constraints and the powered-flight phases was determined. The greater flexibility and superiority of parking-orbit type trajectories over the direct-ascent type was demonstrated. It appears certain that all future lunar and interplanetary trajectories will employ parking orbits. In fact, certain missions *must* employ them; otherwise no mission can occur.

References

[1] Clarke, V. C., Jr., Roth, R. Y., Bollman, W. E., Hamilton, T. H., and Pfeiffer, C. G., "Earth-Venus trajectories, 1964–70," Vols. I–V, Tech. Memo. 33-99, Jet Propulsion Lab., Pasadena, Calif. (October 31, 1962).

[2] Clarke, V. C., Jr., "A summary of the characteristics of ballistic interplanetary trajectories, 1962–77," TR 32-209, Jet Propulsion Lab., Pasadena, Calif. (January 15, 1962).

[3] Clarke, V. C., Jr., Roth, R. Y., Bollman, W. E., Hamilton, T. W., and Pfeiffer, C. G., "Earth-Mars trajectories, 1964–77," Vols. I–VII, Tech. Memo. 33-100, Jet Propulsion Lab., Pasadena, Calif. (to be published).